Methoxo-bridged diiron(III) complex of *m*-xylylenebis(acetylacetonate) showing remarkable thermal stability for encapsulated dichloromethane†

Supriya Dutta,*[a] Papu Biswas,[a] Sujit K. Dutta[b] and Kamalaksha Nag*[a]

Received (in Montpellier, France) 21st October 2008, Accepted 28th November 2008
First published as an Advance Article on the web 27th January 2009
DOI: 10.1039/b818578f

The synthesis, structural characterization, spectroscopic, magnetic, electrochemical and thermal properties of a methoxo-bridged dinuclear iron(III) inclusion compound $[Fe_2(m\text{-xba})_2(\mu\text{-}OCH_3)_2]\cdot CH_2Cl_2$ (**1**) derived from *m*-xylylenebis(acetylacetone) $H_2(m\text{-xba})$ are reported. In **1**, the symmetry related two distorted octahedral iron(III) centres are separated by 3.164(8) Å and the distance between the centroids of the aromatic ring planes is 11.836 Å. In the solid state molecular association takes place through C–H···O and C–H···Cl types of hydrogen bondings leading to the remarkable thermal stability of **1** whose desolvation takes place between 140 and 220 °C. The enthalpy change due to the loss of dichloromethane, as determined by differential scanning calorimetric measurement, is −103 kJ mol^{-1}. Variable-temperature (4–300 K) magnetic susceptibility measurements indicated antiferromagnetic exchange interaction ($H = -2JS_1S_2$) in **1** with $J = -13.5$ cm^{-1}. The ^1H NMR spectrum of **1** in CD_2Cl_2 is consistent with its symmetric structure and exhibits maximum paramagnetic shift for the methoxy protons (*ca.* 200 ppm). The cyclic voltammogram of **1** in dichloromethane in the potential range 0 to −1.2 V exhibits a quasi-reversible redox couple due to $Fe^{III}Fe^{III}/Fe^{III}Fe^{II}$ with $E_{1/2} = -0.85$ V. Further reduction to the $Fe^{II}Fe^{II}$ state at −1.5 V leads to decomposition of the complex species.

Introduction

A paradigm shift has occurred in studies of coordination chemistry due to the emergence of a wide range of metallo-supramolecular entities that exhibit unusual structures and properties.[1–5] In the generation of metallosupramolecular assemblies and in the manifestation of their properties, aside from the nature of metal–ligand bonds, weaker non-covalent interactions play significant roles.

In a pioneering study, using *m*-xylylenebis(acetylacetone) as a metal receptor, a cofacial dicopper(II) complex $[Cu_2(m\text{-xba})_2]$ was reported in which the two metal centres are separated by 4.908(2) Å.[6] The void space inside the metallacycle was insufficient for *endo*-coordination of Lewis bases. Accordingly, the acetonitriles in $[Cu_2(m\text{-xba})_2(CH_3CN)_2]$ are *exo*-coordinated with the Cu···Cu distance being 4.830(1) Å.[7] On increasing the spacer length by introducing a napthalylene bridge, the dicopper(II) complex $[Cu_2(nba)_2]$ could accommodate two chloroform molecules inside the void space (Cu···Cu = 7.349(1) Å)[8] and also could intramolecularly coordinate bidentate Lewis bases such as pyrazine derivatives (Cu···Cu = 7.480(1) Å)[7] and diazabicyclooctane (Cu···Cu = 7.403(4) Å).[8] Further increase of the void space inside the metallacycle was accomplished by using *m*-terphenyl as the spacer.[9] Indeed, the volume of the empty space (400 $Å^3$) was sufficient to accommodate ten chloroform molecules and accept 4,4′-bipyridine as a guest for *endo*-coordination (Cu···Cu *ca.* 11.80 Å).[9] In contrast to copper(II), both vanadium(II) and vanadium(III) form highly staggered six-coordinate complexes with $(m\text{-xba})^{2-}$. Thus, in $[V^{II}_2(m\text{-xba})_2(tmeda)_2]$ (tmeda = tetramethylethylenediamine) the V···V distance is 11.444(1) Å, while in $[V^{III}_2(m\text{-xba})_2X_2(thf)_2]$ (X = Cl, Br, thf = tetrahydrofuran) the metal centres are *ca.* 11.66 Å apart.[10] In recent years a spate of studies have been reported on self-assembled di-, tri- and tetranuclear metallosupramolecular species for di- and trivalent metals with 1,3- and 1,4-aryl linked bis-β-diketones.[11–16] They have provided supramolecular motifs with flat, helical, triangular and tetrahedral architectures. However, except for those of copper(II) and vanadium(II and III), no further metal complexes of $(m\text{-xba})^{2-}$ were forthcoming. In view of the strong tendency of iron(III) to form oxo-bridged dinuclear complexes, often with the Fe–O–Fe angle close to 180°, we considered that a face-to-face μ-oxo diiron(III) complex might be obtained with $(m\text{-xba})^{2-}$. However, contrary to this expectation, we find that despite the variation of procedures a dimethoxo-bridged complex $[Fe_2(m\text{-xba})_2(\mu\text{-}OCH_3)_2]$ is produced, which with dichloromethane forms an inclusion

[a] *Department of Inorganic Chemistry, Indian Association for the Cultivation of Science, Jadavpur, Kolkata, 700032, India. E-mail: ickn@iacs.res.in*
[b] *Department of Chemistry, Ramananda College, Bishnupur, 722122, India*

† Electronic supplementary information (ESI) available: Observed and simulated ESI-MS spectra of compound **1** (Fig. S1), Proton NMR spectra of compound **1** in CD_2Cl_2 (Fig. S2) and space filling diagram showing void space after removal of CH_2Cl_2 (Fig. S3). CCDC reference number 705788. For ESI and crystallographic data in CIF or other electronic format see DOI: 10.1039/b818578f

compound. This study is concerned with the structure, thermal, magnetic and electrochemical behaviour of $[Fe_2(m\text{-xba})_2(\mu\text{-}OCH_3)_2 \subset CH_2Cl_2]$.

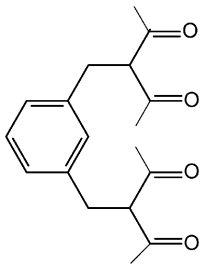

$H_2(m$-xba)

Experimental

Materials

All reagents obtained from commercial sources were used without further purifications. Solvents were purified and dried according to standard methods.[17] The ligand *m*-xylylenebis-(acetylacetone) $H_2(m$-xba) was prepared according to the reported procedure.[18]

Physical measurements

Elemental (C, H and N) analyses were performed on a Perkin-Elmer 2400II elemental analyzer. FTIR (KBr) spectra were recorded on a Shimadzu 8400S spectrometer. Electrospray ionization mass spectra (ESI-MS) were obtained on a Micromass Qtof YA 263 mass spectrometer. The ^{1}H NMR spectra (300 MHz) were recorded on a Bruker Avance DPX-300 spectometer. The UV-Vis spectra were recorded on a Perkin-Elmer Lambda 950 spectrophotometer. Variable-temperature (4–300 K) magnetic susceptibility measurements were carried out using a Quantum Design MPMS SQUID magnetometer under an applied field of 1 T. Experimental susceptibility data were corrected for diamagnetism using Pascal's constants.[19] Thermogravimetric analysis (TGA) was performed on a SDT Q600 thermogravimetric analyzer under flowing nitrogen with the heating rate 5 °C min^{-1}. Differential scanning calorimetric (DSC) measurements were carried out on a Perkin-Elmer Diamond DSC instrument under argon atmosphere with the same heating rate as used for TGA. The enthalpy change due to detrapping of dichloromethane in the inclusion compound was estimated by using the software Pyris 7.0 provided with the instrument. The heat of fusion of indium was used as reference. The cyclic voltammetric (CV) and square wave (SWV) voltammetric measurements were carried out in dichloromethane solution at room temperature under nitrogen atmosphere using a BAS 100B electrochemical analyzer. The solutions were 10^{-3} mol dm^{-3} in the complex and 0.1 mol dm^{-3} in the supporting electrolyte tetrabutylammonium perchlorate (TBAP). The three-electrode assembly comprised of a glassy carbon working electrode, a platinum auxiliary electrode and a Ag/AgCl reference electrode. The reference electrode was separated from the bulk electrolyte by a TBAP salt bridge in acetonitrile. IR compensation was made automatically. Under the experimental condition, the ferrocene–ferrocenium couple was observed at 550 mV.

Preparation of $[Fe^{III}_2(m\text{-xba})_2(\mu\text{-}OCH_3)_2]\cdot CH_2Cl_2$ (1)

To a stirred methanol solution (150 cm^3) of $H_2(m$-xba) (0.60 g, 2 mmol) was added $Fe(ClO_4)_3\cdot 6H_2O$ (0.92 g, 2 mmol) when the solution became purple. On dropwise addition of triethylamine (0.40 g, 4 mmol) diluted with methanol (10 cm^3) to this solution the colour gradually changed to red and eventually a red product began to deposit. After 1 h, the red solid was filtered off and washed successively with methanol and diethyl ether. The product was recrystallized from dichloromethane. Yield 0.73 g (85%). Found: C, 54.55; H, 5.54; Fe, 12.91. $C_{39}H_{48}Cl_2Fe_2O_{10}$ requires: C, 54.48; H, 5.58; Fe, 13.01%. MS (ESI positive in CH_2Cl_2) m/z = 797.4 (100%) $[Fe_2(m\text{-xba})_2(\mu\text{-}OCH_3)_2Na]^+$; 743.3 (40%) $[Fe_2(m\text{-xba})_2(\mu\text{-}OCH_3)]^+$. IR (KBr, ν/cm^{-1}) 1574 (s), 1462 (s), 1367 (s), 1282 (s), 1038 (m), 955 (m), 761 (m), 729 (w), 503 (w), 450 (w). UV-Vis [in dichloromethane, λ_{max}/nm (ε/dm^3 mol^{-1} cm^{-1})] 275 (22500), 440 (4040). ^{1}H NMR (CD_2Cl_2, δ_H/ppm): *ca.* 200 (6H, OCH_3), 17.5 (24H, CH_3), 9.85 (4H, CH_2), 7.59 (2H, Ph), 7.35 (2H, Ph), 7.16 (4H, Ph), 4.88 (4H, CH_2).

An alternative method of preparation involving the use of aqueous sodium hydroxide solution instead of triethylamine, produced a red compound, albeit contaminated with iron(III) hydroxide. Recrystallization of this product twice from dichloromethane afforded **1** in *ca.* 45% yield.

In yet another method, a reaction between $Fe(ClO_4)_2\cdot 6H_2O$ (1 equiv.), $H_2(m$-xba) (1 equiv.) and triethylamine (2 equiv) in methanol was first carried out under nitrogen, following which the solution was stirred in air for 1 h. A brick red product that precipitated was filtered off and recrystallized from dichloromethane. Compound **1** was isolated in *ca.* 30% yield.

X-ray crystallography

Crystals suitable for structure determination $[Fe_2(m\text{-xba})_2(\mu\text{-}OCH_3)_2]\cdot CH_2Cl_2$ (**1**) were obtained by diffusing hexane to a solution of **1** in dichloromethane. Intensity data were collected at 150 K on a Bruker-APEX II SMART CCD diffractometer using graphite-monochromated Mo-Kα radiation (λ = 0.71073 Å). For data processing and absorption correction the packages SAINT[20] and SADABS[20] were used. The structure was solved by direct and Fourier methods and refined by full-matrix least-squares based on F^2 using SHELXTL[20] and SHELXL-97[21] packages. The non-hydrogen atoms were refined anisotropically, while the hydrogen atoms were placed at geometrically calculated positions with a fixed isotropic thermal parameter. The dichloromethane in **1** was disordered and was modelled with the carbon (C20) and one of the chlorine atoms (Cl1) occupying two positions equally (0.5), while the second chlorine atom (Cl2) remains in the fixed position. Crystal data and selected details of structure determination are given in Table 1.

Table 1 Crystallographic data for $[Fe_2(m\text{-xba})_2(\mu\text{-}OCH_3)_2]\cdot CH_2Cl_2$ (**1**)

Formula	$C_{39}H_{48}O_{10}Fe_2Cl_2$
M	859.37
T/K	150(2)
Crystal system	Monoclinic
Space group	$C2/c$
a/Å	22.209(3)
b/Å	10.7792(13)
c/Å	19.506(2)
β/°	123.758(3)
U/Å^3	3882.3(8)
Z	4
D/g cm^{-3}	1.470
μ/mm^{-1}	0.942
$F(000)$	1792
Crystal size/mm	0.12 × 0.16 × 0.22
No. measured reflections	22173
No. observed reflections	3576
R_{int}	0.0832
Parameters refined	251
No. of reflections [$I > 2\sigma(I)$]	2545
Goodness of fit, S^a	1.015
Final R_1,[b] wR_2[c] [$I > 2\sigma(I)$]	0.0500, 0.1137
R_1,[b] wR_2[c] (all data)	0.0795, 0.1286

[a] $S = [\sum w(F_o^2 - F_c^2)^2/(N - P)]^{1/2}$ where N is the number of data and P the total number of parameters refined. [b] $R_1(F) = \sum||F_o| - |F_c||/\sum|F_o|$. [c] $wR_2(F^2) = [\sum w(F_o^2 - F_c^2)^2/\sum w(F_o^2)^2]^{1/2}$.

Results and discussion

Synthesis and characterization

The methoxo-bridged diiron(III) complex $[Fe_2(m\text{-xba})_2(\mu\text{-}OCH_3)_2]$ is readily obtained by reacting $Fe(ClO_4)_3\cdot 6H_2O$ with $H_2(m\text{-xba})$ and $N(C_2H_5)_3$ in the molar ratio 1 : 1 : 2 in methanol solution. As already mentioned, the use of conventional methods for producing hydroxo-bridged or oxo-bridged iron(III) compounds in the present case afforded the methoxo-bridged compound, albeit in reduced yield. On recrystallization from dichloromethane, the solvent inclusion compound $[Fe_2(m\text{-xba})_2(\mu\text{-}OCH_3)_2]\cdot CH_2Cl_2$ (**1**) is obtained in crystalline form. Attempts to obtain inclusion compounds using solvents such as chloroform, dichloromethane and carbon tetrachloride were not successful. Compound **1** does not lose the solvent molecule at room temperature and crystallinity is retained over an indefinitely long period. It may be mentioned that iron(III) tris(acetylacetonate) is long known to form clathrate compounds[22] with chlorinated solvents such as CH_2Cl_2, $CHCl_3$, CCl_4, *trans* ClCH=CHCl *etc*. The X-ray structure of $Fe(acac)_3\cdot CCl_4$[23] and $Fe(acac)_3\cdot C_2H_2Cl_2$[24] have been reported. However, unlike **1**, all these clathrates rapidly lose the solvent molecule when they are removed from mother-liquor.

The IR spectrum of compound **1** exhibits two strong bands at 1574 and 1462 cm^{-1} that are characteristic of metal β-diketonates due to combination stretching vibrations ν(C···C) and ν(C···O).[25] The ESI-MS of **1** (Fig. S1 of ESI†) shows two peaks at m/z = 797.4 (100%) and 743.3 (40%) due to $[Fe_2(m\text{-xba})_2(\mu\text{-}OCH_3)_2Na]^+$ and $[Fe_2(m\text{-xba})_2(\mu\text{-}OCH_3)]^+$, respectively. As shown in Fig. S1, the isotopic distribution patterns of the observed and simulated mass spectra are in excellent agreement. Compound **1** is further characterized by its UV-Vis spectrum in dichloromethane, which displays two bands at 275 (ε = 22500 dm^3 mol^{-1} cm^{-1}) and 440 nm (ε = 4040 dm^3 mol^{-1} cm^{-1}). The band at 275 nm is due to π–π* transition of the ligand, while the peak observed at 440 nm can be attributed to ligand to metal charge transfer transition involving pπ orbitals of the acetylacetonato oxygen and dπ orbitals of iron(III).

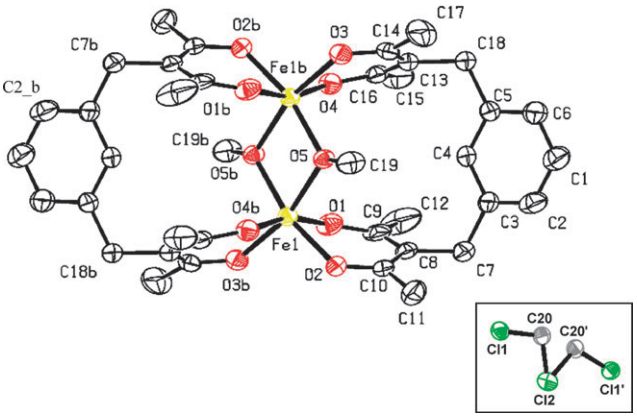

Fig. 1 The ORTEP representation of $[Fe_2(m\text{-xba})_2(\mu\text{-}OCH_3)_2]\cdot CH_2Cl_2$ (**1**) showing 50% probability displacement ellipsoids. Inset shows the disordered CH_2Cl_2. Symmetry transformations used to generate equivalent b atoms and the disordered CH_2Cl_2 in **1** are 1/2 − x, 1/2 − y, 1 − z and −x, y, 1/2 − z, respectively.

Description of crystal structure

Complex $[Fe_2(m\text{-xba})_2(\mu\text{-}OCH_3)_2]\cdot CH_2Cl_2$ (**1**) crystallized in the monoclinic form with $C2/c$ space group. The structural representation of **1** is shown in Fig. 1 and a selection of bond distances and angles are listed in Table 2. In **1**, each of the two iron centres are coordinated by two acetylacetonate units of each half parts of the two $(m\text{-xba})^{2-}$ ligands and the two metal centres are bridged by the two methoxide oxygens (O5) and (O5′). The four atoms of the $Fe_2(\mu\text{-}OCH_3)_2$ diamond-core are coplanar and the inversion centre of **1** is located at the midpoint of this core. For the pseudo-octahedral FeO_6 chromophore, the equatorial plane is provided by the atoms O(2) O(3) O(5) O(5′), while O(1) and O(4) occupy the axial positions. From the mean basal plane the constituent atoms are displaced by 0.076 to 0.098 Å. The two FeO_6 octahedra share a common edge provided by O(5) and O(5′). All the Fe–O

Table 2 Selected bond lengths (Å) and angles (°) for $[Fe_2(m\text{-xba})_2(\mu\text{-}OCH_3)_2]\cdot CH_2Cl_2$ (**1**)[a]

Fe–O(1)	2.000(3)	Fe–O(4)	1.990(3)
Fe–O(2)	1.996(3)	Fe–O(5)	1.990(2)
Fe–O(3)	1.986(3)	Fe–O(5′)	1.997(2)
Fe(1)···Fe(1′)	3.164(8)	O(5)···O(5′)	2.427(8)
O(1′)–Fe–O(2′)	83.36(11)	O(2′)–Fe–O(5′)	91.51(10)
O(1′)–Fe–O(3)	86.94(11)	O(3)–Fe–O(4)	84.31(11)
O(1′)–Fe–O(4)	163.27(11)	O(3)–Fe–O(5)	90.85(11)
O(1′)–Fe–O(5)	93.30(10)	O(3)–Fe–O(5′)	164.67(11)
O(1′)–Fe–O(5′)	99.42(11)	O(4)–Fe–O(5)	101.05(10)
O(2′)–Fe–O(3)	103.13(11)	O(4)–Fe–O(5′)	92.64(10)
O(2′)–Fe–O(4)	84.77(11)	O(5)–Fe–O(5′)	74.95(11)
O(2′)–Fe–O(5)	165.38(10)	Fe(1)–O(5)–Fe(1′)	105.05(11)

[a] Symmetry transformation used to generate equivalent (primed) atoms: 1/2 − x, 1/2 − y, 1 − z.

distances in FeO_6 are closely similar, ranging between 1.990(3) and 2.000(3) Å. In contrast, the O–Fe–O angles are quite dissimilar. For instance, the *cis* angles vary from 83.4(11) to 103.1(11)°, while the *trans* angles lie between 163.3(11) and 165.4(11)°. Thus, there is considerable distortion from ideal octahedral geometry. The Fe–O(5)–Fe′ and O(5)–Fe–O(5′) angles of the diamond-core are 105.05(11) and 74.95(11)°, respectively. While the nonbonding Fe···Fe′ and O(5)···(O5′) distances are 3.164(8) and 2.427(8) Å, the aromatic ring-planes are parallel and the distance between their centroids is 11.836 Å.

As already mentioned, the dichloromethane in **1** is disordered, the carbon and one of the chlorine atoms occupy two positions equally, while the second chlorine remains in a fixed position (shown in the inset of Fig. 1). Unconventional C–H···O/Cl types of hydrogen bonds play important roles for supramolecular assembling of **1** in the solid state.[26] There are three intermolecular hydrogen bridges involving either an aromatic or a methylene C–H and a diketonate oxygen or a chlorine atom of the trapped solvent. Indeed, the involvement of CH_2Cl_2 in hydrogen bonding in two ways, *viz.* C(2)–H(2)···Cl(1) and C(20)–H(20)···O(3) contribute significantly to enhance the thermal stability of **1** towards solvent release. Table 3 lists the relevant hydrogen bonds and the metrical parameters involved therein.

The packing diagram of **1** viewed along the [001] plane (Fig. 2) shows how intermolecular association through hydrogen bonding and van der Waals interaction generate a hollow space in which the disordered solvent molecule CH_2Cl_2 is trapped. The space filling diagram of the supramolecular assembly bereft of the solvent molecule is shown in Fig. S3 (ESI†). Using SQUEEZE of PLATON,[27] the solvent accessible void space has been estimated to be 425.2 $Å^3$ and the electron count per unit cell turns out to be 162, which matches with that of four CH_2Cl_2 molecules present in the unit cell.

Proton NMR spectrum

The hyperfine-shifted proton NMR spectrum of **1** in CD_2Cl_2 (Fig. S2 in ESI†) shows the presence of seven signals at *ca.* 200, 17.5, 9.85, 7.59. 7.35, 7.16 and 4.88 ppm. The most downfield shifted signal, which is very broad and spans over the range 250 to 150 ppm, must be due to the methoxo-bridged protons that have closest proximity to the paramagnetic metal centres. The resonance centered at 17.5 ppm is also quite broad (23–12 ppm) and its integral corresponds to the presence of twenty four protons, indicating it to be due to the eight equivalent methyl groups in the molecule. The three resonances at 7.59, 7.35 and 7.16 ppm that are clustered together have intensity ratios 1 : 1 : 2 and can be attributed to the protons of the phenyl ring located at C(4), C(1) and C(2,6), respectively. The remaining two signals at 9.85 and 4.88 ppm can be attributed to the diastereotopic CHH′ protons of C(7)/C(18).

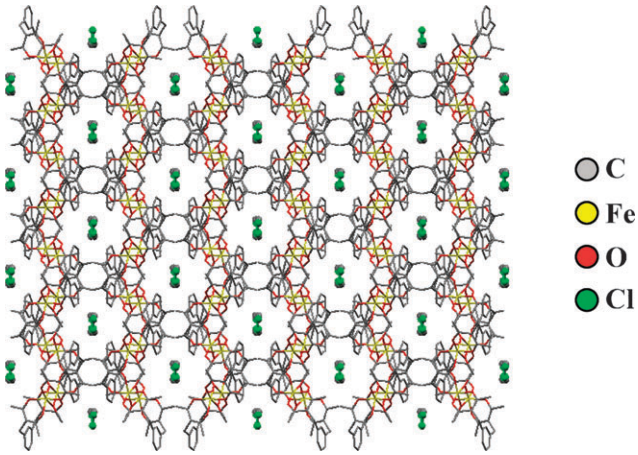

Fig. 2 A wireframe projection of the crystal packing diagram of $[Fe_2(m\text{-xba})_2(\mu\text{-}OCH_3)_2]\cdot CH_2Cl_2$ (**1**) viewed along the [001] plane.

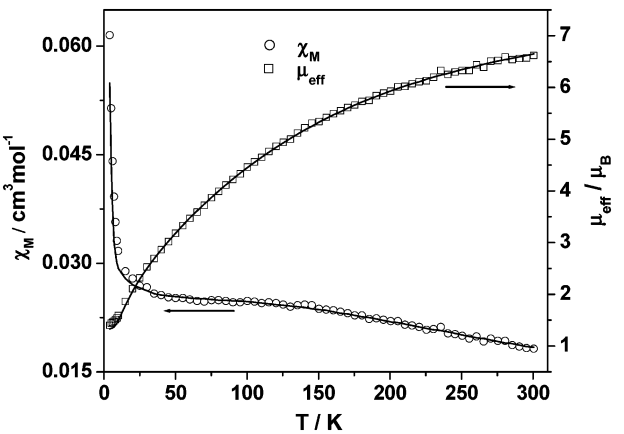

Fig. 3 Molar magnetic susceptibility (○) and effective magnetic moment (□) *vs.* temperature for $[Fe_2(m\text{-xba})_2(\mu\text{-}OCH_3)_2]\cdot CH_2Cl_2$ (**1**). The solid lines result from a least-squares fit.

Magnetism

Variable-temperature magnetic susceptibility measurements for **1** have been carried out between 4 and 300 K. The plots of χ_M and μ_{eff} *vs.* *T* are shown in Fig. 3. The magnetic moment decreases from about 6.7 μ_B at 300 K to *ca.* 1.3 μ_B at 4 K, indicating rather weak antiferromagnetic interaction between two $S = 5/2$ centres. At room temperature, for two non-interacting high-spin iron(III) the calculated spin only magnetic moment is 8.37 μ_B. In terms of the isotropic spin Hamiltonian

Table 3 Hydrogen bond distances (Å) and angles (°) for $[Fe_2(m\text{-xba})_2(\mu\text{-}OCH_3)_2]\cdot CH_2Cl_2$ (**1**)

D–H···A	D–H	H···A	D···A	D–H···A	Symmetry[a]
C(18)–H(18B)···O(2)	0.99	2.53	3.359(6)	141	$x, 1 - y, z - 1/2$
C(20)–H(20)···O(3)	1.00	2.43	3.392(4)	162	
C(2)–H(2)···Cl(1)	0.95	2.67	3.442(6)	138	$1/2 + x, 3/2 - y, 1/2 + z$

[a] Symmetry relation between D and A atoms.

($H = -2JS_1S_2$, with $S_1 = S_2 = 5/2$), excellent least-squares fits have been obtained for the χ_M, T and μ_{eff}, T data with $J = -13.5\ cm^{-1}$, $g = 1.990$, p (mole fraction of mononuclear impurity) = 0.016 and the agreement factor $R = 3 \times 10^{-4}$ ($R = [\sum(\chi_{obs} - \chi_{calc})^2/(\sum\chi_{obs})^2]^{1/2}$). The structural and magnetic properties of several dimethoxo-bridged iron(III) complexes have been reported.[28–31] The Fe···Fe distance in these compounds range between 3.14 and 3.21 Å, while the Fe–O–Fe angle varies from 102.5 to 106.8°. In all cases antiferromagnetic exchange interactions have been reported with the $-J$ values lying in the range 5.7 to 16.3 cm^{-1}. By comparison, for compound **1**, Fe···Fe′ = 3.164(8) Å, Fe–O–Fe = 104.97(10)° and $-J = 13.5\ cm^{-1}$.

Electrochemistry

The redox behavior of complex **1** was studied in dichloromethane using glassy carbon as the working electrode. Fig. 4(a) shows the cyclic voltammogram of **1** in the potential range 0 to −1.2 V at a scan rate of 500 mV s^{-1}. The lone quasi-reversible response observed with $E_{1/2} = -0.85$ V and $\Delta E_p = 0.15$ V is clearly due to the $[Fe^{III}(\mu\text{-}OCH_3)_2Fe^{III}(m\text{-xba})_2]/[Fe^{III}(\mu\text{-}OCH_3)_2Fe^{II}(m\text{-xba})_2]^-$ redox couple. However, when the potential window is extended up to −1.80 V, two cathodic responses are observed at $E_{p.c} = -0.92$ and −1.50 V (shown in Fig. 4(b)), while in the return sweep the anodic waves are observed at $E_{p.a} = -0.84$ and −0.51 V. It appears that the diiron(II) species $[Fe^{II}(\mu\text{-}OCH_3)_2Fe^{II}(m\text{-xba})_2]^{2-}$ generated on the second electron transfer is chemically unstable on the cyclic voltammetric time-scale. As a result, the anodic responses that are observed are unrelated to the generation of the mixed-valent and diiron(III) species.

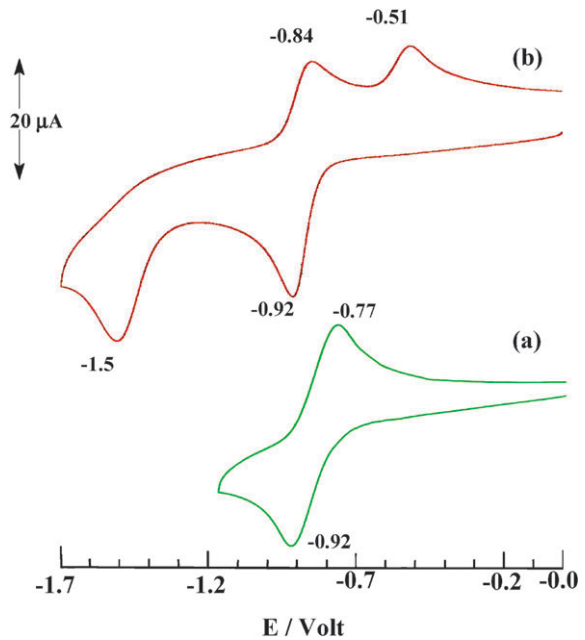

Fig. 4 Cyclic voltammograms of $[Fe_2(m\text{-xba})_2(\mu\text{-}OCH_3)_2]\cdot CH_2Cl_2$ (**1**) in dichloromethane: (a) 0 to −1.7 V and (b) 0 to −1.2 V. For both cases the scan rate was 500 mV s^{-1}.

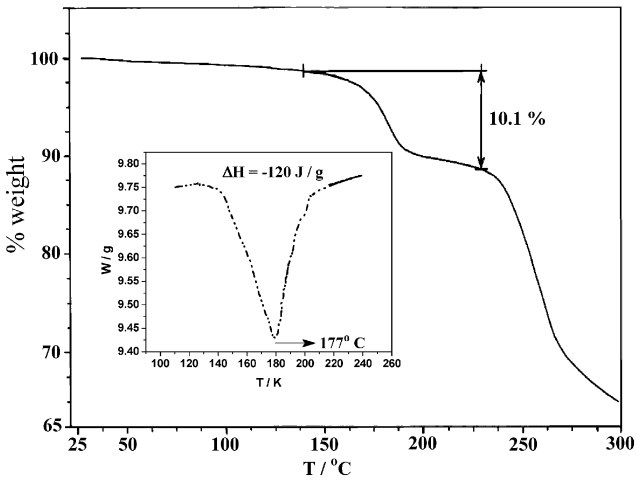

Fig. 5 Thermogravimetric analysis (TGA) of $[Fe_2(m\text{-xba})_2(\mu\text{-}OCH_3)_2]\cdot CH_2Cl_2$ (**1**) in the temperature range 25–300 °C under flowing nitrogen at a heating rate of 5 °C min^{-1}. Inset shows the endothermic loss of CH_2Cl_2 from **1** in DSC measurement carried over the temperature range 25–250 °C under argon atmosphere at a heating rate of 5 °C min^{-1}.

Thermal analysis

The thermogravimetric analysis (TGA) and differential scanning calorimetric (DSC) measurements of $[Fe_2(m\text{-xba})_2(\mu\text{-}OCH_3)_2]\cdot CH_2Cl_2$ (**1**) were carried out under a nitrogen/argon atmosphere with a heating rate 5 °C min^{-1}. As shown in Fig. 5, a weight loss of 10.1% takes place between 140 and 220 °C in the TGA, which is in excellent agreement with the calculated value (9.91%) for loss of one dichloromethane molecule from **1**. The DSC profile (inset of Fig. 5) shows that the endotherm spanning over the range 140 to 220° has its peak at 177 °C. The enthalpy change (ΔH) due to the loss of the solvent molecule is −120 J g^{-1}, that is, −103 kJ mol^{-1}. It should be noted that dichloromethane, with a boiling point at 40 °C has the standard enthalpy change of vaporization $\Delta H^\circ_{vap} = 28$ kJ mol^{-1} (ref. 32). The remarkable thermal stability of **1** with regard to the loss of the solvent molecule is associated with the cage structure that is provided by the intermolecular hydrogen bonds and van der Waals interactions to trap the solvent molecule. It appears that two particular hydrogen bonds, namely C(2)–H(2)···Cl(1) [3.44 Å] and C(20)–H(20)···O(3) [3.39 Å] play significant roles to anchor dichloromethane in the crystal lattice.

Conclusion

Although it was expected that the ligand $(m\text{-xba})^{2-}$ would react with an iron(III) salt to form a cofacial dimeric oxo-bridged compound $[Fe_2(m\text{-xba})_2(\mu\text{-O})]$, a dimethoxo-bridged compound $[Fe_2(m\text{-xba})_2(\mu\text{-}OCH_3)_2]\cdot CH_2Cl_2$ (**1**) has been isolated instead. On hindsight we recognize that since in the oxo-bridged iron(III) complexes Fe–O(oxo) distances range from 1.73 to 1.82 Å,[33] to form a cofacial μ-oxo complex the separation between the two iron(III) centres should not exceed 3.65 Å. However, in the cofacial dicopper(III) complexes $[Cu_2(m\text{-xba})_2]$[6] and $[Cu_2(m\text{-xba})_2(CH_3CN)_2]$[7] the Cu···Cu distances are 4.91 and 4.83 Å, respectively. Clearly, the spacer of the ligand is too long to allow the two flat metal

coordinated β-diketonate units to approach a distance close to 3.65 Å. The remarkable thermal stability of **1** with regard to the loss of dichloromethane seems to be associated with the intermolecular hydrogen bonds C(2)–H(2)···Cl(1) and C(20)–H(20)···O(3). It has been reported recently that desorption of dichloromethane and chloroform adsorbed on a porous framework based on a polymeric zinc(II) complex[34] completes at a temperature of about 70 °C above their boiling points. In the case of **1** the onset of desolvation of dichloromethane occurs at 140 °C and completes at 220 °C, which to our knowledge is unprecedented.

Acknowledgements

K. N. in thankful to the Indian National Science Academy for supporting him as INSA Senior Scientist and SD is grateful to CSIR, India for providing a research fellowship. Thanks are also due to the Department of Science and Technology, Government of India for establishing the National X-ray Diffractrometer facility at the Department of Inorganic Chemistry, Indian Association for the Cultivation of Science. We thank Dr G. Mostafa for his help to sort out a crystallographic problem.

References

1 J.-M. Lehn, *Supramolecular: Chemistry Concepts and Perspectives*, VCH, Weinheim, 1995.
2 S. Leininger, B. Olenyuk and P. J. Stang, *Chem. Rev.*, 2000, **100**, 853; G. F. Swiegers and T. J. Malefeste, *Chem. Rev.*, 2000, **100**, 3483.
3 L. F. Lindoy and I. M. Atkinson, *Self-Assembly in Supramolecular Systems*, Royal Society of Chemistry, Cambridge, UK, 2000.
4 *Supramolecular Chemistry*, ed. J. W. Steed and J. L. Atwood, John Wiley & Sons, Chichester, 2000.
5 S. L. James, *Chem. Soc. Rev.*, 2003, **32**, 276; L. Brammer, *Chem. Soc. Rev.*, 2004, **33**, 476; M. D. Pluth and K. N. Raymond, *Chem. Soc. Rev.*, 2007, **36**, 161.
6 A. W. Maverick and F. Klavetter, *Inorg. Chem.*, 1984, **23**, 4129.
7 A. W. Maverick, D. R. Billodeaux, M. L. Ivie, F. R. Fronczek and E. F. Maverick, *J. Inclusion Phenom. Macrocyclic Chem.*, 2001, **39**, 19.
8 A. W. Maverick, S. C. Buckingham, Q. Yao, J. R. Bradbury and G. G. Stanley, *J. Am. Chem. Soc.*, 1986, **108**, 7430.
9 G. J. E. Davidson, A. J. Baer, A. P. Cote, N. J. Taylor, G. S. Hanan, Y. Tanaka and M. Watanabe, *Can. J. Chem.*, 2002, **80**, 496.
10 P. J. Bonitatebus, Jr., S. K. Mandal and W. H. Armstrong, *Chem. Commun.*, 1998, 939.
11 V. A. Grillo, E. J. Seddon, C. M. Grant, G. Aromi, J. C. Bollinger, K. Folting and G. Christou, *Chem. Commun.*, 1997, 1561.
12 M. Matsushita, T. Yasuda, R. Kawano, T. Kawai and T. Iyoda, *Chem. Lett.*, 2000, 812.
13 J. K. Clegg, L. F. Lindoy, B. Moubaraki, K. S. Murray and J. C. McMurtrie, *Dalton Trans.*, 2004, 2417; J. K. Clegg, L. F. Lindoy, J. C. McMurtrie and D. Schilter, *Dalton Trans.*, 2005, 857; J. K. Clegg, L. F. Lindoy, J. C. McMurtrie and D. Schilter, *Dalton Trans.*, 2006, 3114; J. K. Clegg, K. Gloe, M. J. Hayter, O. Kataeva, L. F. Lindoy, B. Moubaraki, J. C. McMurtrie, K. S. Murray and D. Schilter, *Dalton Trans.*, 2006, 3977.
14 A. P. Bassett, S. W. Magennis, P. B. Glover, D. J. Lewis, N. Spencer, S. Parsons, R. M. Williams, L. De Cola and Z. Pikramenou, *J. Am. Chem. Soc.*, 2004, **126**, 9413.
15 D. J. Bray, J. K. Clegg, L. F. Lindoy and D. Schilter, *Adv. Inorg. Chem.*, 2007, **59**, 1.
16 J. K. Clegg, D. J. Bray, K. Gloe, K. Gloe, M. J. Hayter, K. A. Jolliffe, G. A. Lawrance, G. V. Meehan, J. C. McMurtrie, L. F. Lindoy and M. Wenzel, *Dalton Trans.*, 2007, 1719.
17 D. D. Perrin, W. L. Armarego and D. R. Perrin, *Purification of Laboratory Chemicals*, Pergamon, Oxford, 2nd edn, 1980.
18 A. W. Maverick, D. P. Martone, J. R. Bradbury and J. E. Nelson, *Polyhedron*, 1989, **8**, 1549.
19 C. J. O'Connor, *Prog. Inorg. Chem.*, 1979, **2**, 204.
20 *SAINT, version 6.02; SADABS version; 2.03; SHELXTL, version 6.10*, Madison, Wisconsin, 2002.
21 G. M. Sheldrick, *SHELXL-97, Program for the Refinement of Crystal Structures*, University of Göttingen, Göttingen, Germany.
22 J. F. Steinbach and J. H. Bruns, *J. Am. Chem. Soc.*, 1958, **80**, 1838.
23 L. Pang, E. A. C. Lucken and G. Bernardinelli, *J. Am. Chem. Soc.*, 1990, **112**, 8754.
24 L. Pang, R. C. Hynes and M. A. Whitehead, *Acta Crystallogr., Sect. C*, 1992, **48**, 1594.
25 K. Nakamoto, *Infrared and Raman Spectra of Inorganic and Coordination Compounds*, VCH-Wiley, New York, 5th edn, 1997.
26 G. R. Desiraju and T. Steiner, *The Weak Hydrogen Bond in Structural Chemistry and Biology*, Oxford University Press, Oxford, 1999..
27 A. L. Spek, PLATON, *Acta Crystallogr., Sect. A*, 1990, **46**, C34.
28 B. Chari, O. Piovesana, T. Tarantelli and P. F. Zanazzi, *Inorg. Chem.*, 1982, **21**, 1396; B. Chari, O. Piovesana, T. Tarantelli and P. F. Zanazzi, *Inorg. Chem.*, 1982, **21**, 2444; B. Chari, O. Piovesana, T. Tarantelli and P. F. Zanazzi, *Inorg. Chem.*, 1984, **23**, 3398.
29 A. Caneschi, A. Cornia, A. C. Fabretti, S. Foner, D. Gatteschi, R. Grandi and L. Schenetti, *Chem.–Eur. J.*, 1996, **200**, 1379; G. L. Abbati, A. Caneschi, A. Cornia, A. C. Fabretti, D. Gatteschi, W. Malavasi and L. Schenetti, *Inorg. Chem.*, 1997, **36**, 6443; A. Cornia, M. Affronte, A. G. M. Janesen, G. L. Abbati and D. Gatteschi, *Angew. Chem., Int. Ed.*, 1999, **38**, 2264; G. L. Abbati, A. Caneschi, A. Cornia, A. C. Fabretti and D. Gatteschi, *Inorg. Chim. Acta*, 2000, **297**, 291.
30 P. Baran, A. Böttcher, H. Elias, W. Haase, M. Hüber, H. Fuess and H. Paulus, *Z. Naturforsch., B*, 1992, **47**, 1681.
31 F. Banse, V. Balland, C. Philouze, E. Riviere, L. Tchertanova and J.-J. Girerd, *Inorg. Chim. Acta*, 2003, **353**, 223.
32 *CRC Handbook of Chemistry and Physics*, 47th edn, CRC Press, Ann Arbor, MI.
33 D. M. Kurtz, Jr., *Chem. Rev.*, 1990, **90**, 585.
34 X. Lin, A. J. Blake, C. Wilson, X. Z. Sun, N. R. Champness, M. W. George, P. Hubberstey, R. Mokaya and M. Schröder, *J. Am. Chem. Soc.*, 2006, **128**, 10745.

